RSC Advances

Effects of Heavy Metal Ions on N-Nitrosodimethylamine (NDMA) Formation

Journal:	*RSC Advances*
Manuscript ID	RA-ART-05-2016-011481.R1
Article Type:	Paper
Date Submitted by the Author:	13-Jul-2016
Complete List of Authors:	Liu, Yameng; Beijing University of Technology, College of Life Science and Bioengineering; University of Georgia, Computational Chemistry Liu, Yongdong; Beijing University of Technology, College of Life Science and Bioengineering zhong, ru-gang; Beijing University of Technology, PENG, BIN; University of Georgia, Computational Chemistry; Center for Computational Quantum Chemistry, MOE Key Laboratory of Theoretical Chemistry of the Environment, South China Normal University Schaefer, Henry; University of Georgia, Computational Chemistry
Subject area & keyword:	Computational - Chemical biology & medicinal < Chemical biology & medicinal

Effects of Heavy Metal Ions on *N*-Nitrosodimethylamine (NDMA) Formation

Yameng Liu,[ac] Yongdong Liu,*[a] Rugang Zhong,[a] Bin Peng,*[bc]

Henry F. Schaefer, III*[c]

[a] Beijing Key Laboratory of Environmental and Viral Oncology, College of Life Science & Bioengineering, Beijing University of Technology, Beijing 100124, P. R. China

[b] Center for Computational Quantum Chemistry, MOE Key Laboratory of Theoretical Chemistry of the Environment, South China Normal University, Guangzhou, Guangdong 510631, P. R. China

[c] Center for Computational Quantum Chemistry, University of Georgia, Athens, Georgia 30602, United States

[a]Corresponding author. E-mail: ccq@uga.edu.

[b]Corresponding author. E-mail: ydliu@bjut.edu.cn.

[c] Corresponding author. E-mail: pengbin@scnu.edu.cn.

Abstract

Heavy metals as pollutants cause threats to the environment and human health. Nitrosodimethylamine (NDMA) is a probable human carcinogen. In this research, the mechanism of NDMA formation as affected by heavy metal complexes $[MONO]^+$ (M=Cd, Pb, Hg) was investigated using density functional theory (DFT). The results show that the formation of NDMA from the reaction of DMA with NO_2^- can be catalyzed by the heavy metal complex. Three possible NDMA formation pathways are obtained. Moreover, we find that one molecule of $[MONO]^+$ (Pathway 1, M=Cd, Hg; Pathway 2, M=Cd, Pb, Hg) reacts directly with DMA via two different pathways, forming different transition states to produce NDMA. Another mechanism (Pathway 3) shows that two $[CdONO]^+$ molecules will produce N_2O_3 which reacted with DMA to give NDMA. These findings will expand our understanding of the environmental significance of heavy metal ions and perhaps help develop efficient methods to prevent the formation of carcinogenic nitrosamines.

1. Introduction

Nitrosamines are a class of undesirable industrial and environmental pollutants which are carcinogenic, mutagenic, and teratogenic.[1,2] The simplest dialkylnitrosamine, *N*-nitrosodimethylamine (NDMA) has been demonstrated as a cause of cancers in several organs including liver, lung, and kidney.[3,4] Because of their toxicity to animals and their ubiquity in the environment, understanding the mechanisms by which NDMA are formed is of importance.

NDMA has been found in air, soil, water, food, cosmetics, rubber products, and many other materials.[5-8] Formation mechanisms of NDMA in wastewater or drinking water have been widely studied and recently reviewed.[9,10] It is believed that a chloramination mechanism, suggested by Valentine and Mitch, is likely the most important NDMA formation mechanisms during water treatment.[11 - 14] Pathways including ozonation, chlorine-nitrite, breakpoint chlorination, activated carbon and photolysis are also possible under certain conditions.[15-21]

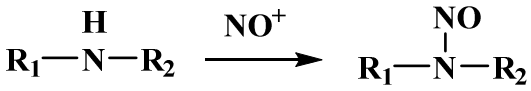

Scheme 1. The nitrosation reaction

As shown in scheme 1, the nitrosation of a secondary amine is a well-known synthetic path to nitrosamine in the laboratory.[22] It is found that NDMA can be formed by this way in the stomach where the nitrosation reaction is favored by acid

conditions[23–27]. Nitrosation involving different nitrosating agents N_2O_4, NO and NO_2 has been studied theoretically. [28-31]

Although nitrosation is thought to be an acid catalyzed reaction, it is found that various secondary amines are converted to nitrosamines, when catalyzed by formaldehyde in the pH range 6~11. [32] Previous theoretical research found that CO_2 could catalyze the formation of NDMA when the weak nitrosating agents NO_2^- or NO_3^- are involved.[33,34] Recently, aqueous copper released from malachite [$Cu_2CO_3(OH)_2$] has been shown to promote NDMA formation.[35] Further research suggests that the catalytic effects of Cu is associated with the oxidative degradation of primary amines.[36] Since heavy metal ions like Pb^{2+}, Hg^{2+}, Cd^{2+} are widely used in various products and can enter into the human body through consumption of contaminated food, drinking water or the inhalation of dust, [37] it is reasonable to conclude that the metal ions Pb^{2+}, Hg^{2+}, Cd^{2+} or their complexes will be involved in the NDMA formation process. Complexes $[MONO]^+$ (M=Cd, Pb, Hg) may be formed by metal ion M^{2+} and nitrite anion or nitrous acid in solution. Here reaction mechanisms of NDMA formation in the presence of $[MONO]^+$ (M=Cd, Pb, Hg) are investigated theoretically. The conclusions will be helpful for understanding the effects of heavy metal ions on nitrosamine formation.

2. Computational Methods

All structures of reactants, transition states, intermediates, and products were fully optimized using the B3LYP method (Becke's three-parameter nonlocal exchange functional [38] with the correlation functional of Lee, Yang, and Parr [39]) with the

6-311+G(d,p) basis set[40,41] for C, H, O N atoms. For Cu, Hg, Pb, the numbers of electrons increase the required computational resources. In order to reduce the cost, we employed effective core potential (ECP) relativistic basis sets, namely LANL2DZ,[42] for the heavy metal atoms. Vibrational frequencies were computed at the same level of theory to characterize the nature of the stationary points. Intrinsic Reaction Coordinate (IRC) studies were performed to confirm that every transition state connects with the corresponding reactant and product through the minimum-energy pathway. Natural atomic charges[43] are obtained at same level of theory in order to discuss the charge distributions of the entrance complexes, intermediates and transition states on all pathways. All the computations presented here were carried out with the Gaussian 09 program package.[44]

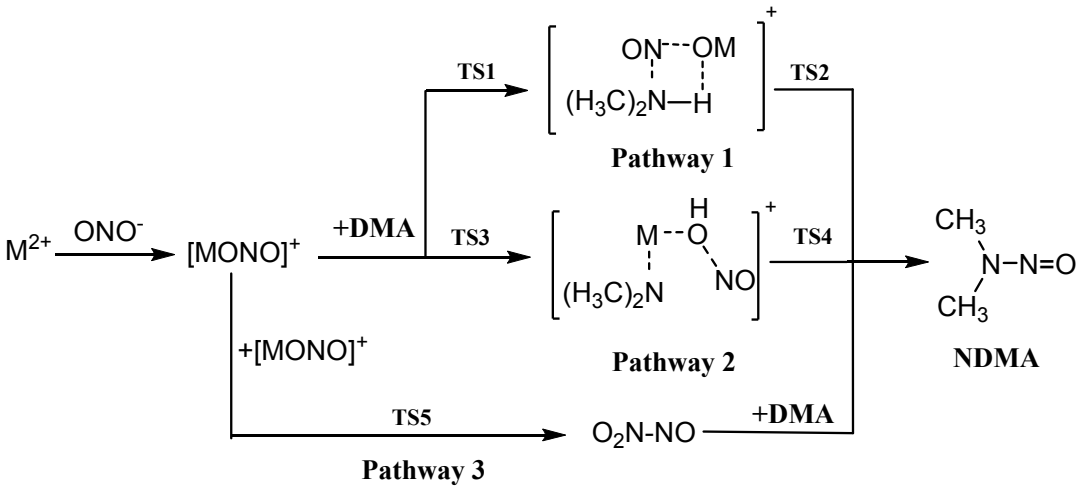

Scheme 2. NDMA formation pathways in the presence of heavy metal ions M^{2+} (M = Cd, Pb, Hg)

3. Results and Discussion

As illustrated in Scheme 2, both Pathway 1 and 2 are NDMA formation mechanisms from $[MONO]^+$ (Pathway 1, M=Cd, Hg; Pathway 2, M=Cd, Pb, Hg) and DMA. Following pathway 3, two $[CdONO]^+$ molecules will produce N_2O_3 which was suggested by previous research [34] to react with DMA giving NDMA. Reaction energies ΔH_{298K}, ΔG_{298K} (in kcal/mol) of all pathway are reported in Table 1.

Table 1. Reaction energy (in kcal/mol) obtained at B3LYP/6-311+G(d,p)/LANL2DZ level in gas phase

Reactions	ΔH_{298K}	ΔG_{298K}
$DMA+[CdONO]^+ \rightarrow NDMA + CdOH^+$ (Pathway 1)	3.9	3.2
$DMA+[HgONO]^+ \rightarrow NDMA + HgOH^+$ (Pathway 1)	10.0	11.1
$DMA+[CdONO]^+ \rightarrow NDMA + CdOH^+$ (Pathway 2)	22.4	21.5
$DMA+[HgONO]^+ \rightarrow NDMA + HgOH^+$ (Pathway 2)	22.6	24.0
$DMA+[PbONO]^+ \rightarrow NDMA + PbOH^+$ (Pathway 2)	6.1	7.5
$2[CdONO]^+ \rightarrow N_2O_3 + Cd_2O^{2+}$ (Pathway 3)	-17.6	-17.7

3.1 The Formation of NDMA from DMA and $[MONO]^+$(M=Cd, Hg), Pathway 1

The stepwise reaction mechanism leading to NDMA is favored when the effects of Cd^{2+} and Hg^{2+} on DMA were taken into consideration. The reaction between DMA and $[PbONO]^+$ can not follow this pathway. As shown in Scheme 2, this mechanism includes two steps: (1) formation of an Intermediate from the reactions of DMA and $[MONO]^+$; and (2) formation of NDMA from the noted Intermediate. The relative energies and

optimized geometry of stationary points on this pathway are shown in Figure 1. Since TS1, the Intermediate and TS2 are structurally similar, they are all presented as part of the same picture in Figure 1.

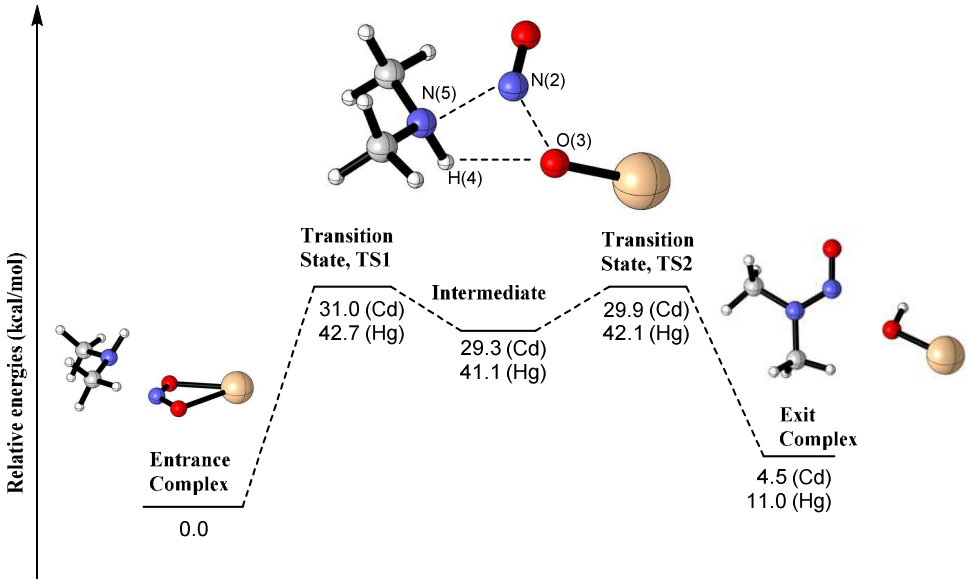

Figure 1 Stationary points for Pathway 1 of the DMA + $[MONO]^+$ (M=Cd, Hg) reaction

As shown in Figure 1, DMA and $[MONO]^+$ are connected by the N(2)–N(5) bond, with distances 2.02 (Cd) or 1.99 (Hg) Å, respectively. In the meantime, $[MONO]^+$ breaks into two fragments, namely NO and MO^+; the corresponding distances between N(2) and O(3) are 1.87 (Cd) or 1.95 (Hg) Å, respectively. The distances between atoms O(3) and H(4) are longer than 2.15 Å, suggesting a weak interaction between them.

The energy of the discovered intermediate is 1.7 (Cd) or 1.5 (Hg) kcal/mol lower in energy than TS1. The N(2)–N(5) bond length are 1.97 (Cd) or 2.00 (Hg) Å, respectively, which are barely changed compared with TS1. On the other hand, the N(2)-O(3) bonds are elongated 0.25 (Cd) or 0.15 (Hg) Å compared with TS1. The distances between O(3)

and H(4) are 1.84 (Cd) or 1.92 (Hg) Å, respectively, suggesting a hydrogen bond interaction between MO and DMA.

As shown in Figure 1, the second transition state in pathway 1, namely TS2, follows the Intermediate with a few geometry changes. The N(2)–N(5) bond is ~1.82 Å, shortened by 0.15 (Cd) or 0.18 (Hg) Å , relative to their values in the Intermediate. The N(2)–O(3) distances are elongated to 2.53 (Cd) or 2.63 (Hg) Å. The hydrogen atom H(4) from DMA bond to MO^+ (M=Cd, Hg) forming an O(3)–H(4) connection with distances 1.48 (Cd) or 1.50 Å, respectively. In the meantime, H(4) atom still connected with DMA, the corresponding H(4)–N(5) bond elongated to 1.08 (Cd) or 1.07 (Hg) Å, respectively.

Thus, following this pathway, $[MONO]^+$ from entrance complex break into $[MO]^+$ and NO which attached to DMA molecule by forming N(2)–N(5) bond. Simultaneously, oxygen atom O(3) from MO^+ removes hydrogen atom H(4) from DMA to form $[MOH]^+$ which will finally dissociate to produce NDMA.

From Figure 1, the energy barriers to produce the Intermediate are predicted to be 31.0 (Cd) or 42.7 kcal/mol (Hg), respectively, implying the energies required to break N–O bond in $[MONO]^+$. Moreover the reaction of DMA with $[CdONO]^+$ is energetically preferred vis-à-vis the reaction of DMA with $[HgONO]^+$ to generate the transition state, TS1. Thus Cd^{2+} is preferable to Hg^{2+} for this reaction system. It is reasonable that energy differences between TS1, the Intermediate, and TS2 are less than 2 kcal/mol, considering that these three complexes are similar to each other in geometry. The main geometrical change along these steps are formation of N(2)–N(5), O(3)–H(4) bonds and elongation of

N(5)–H(4) bond. Moreover, the two reactions, from entrance complex to exit complex, are endothermic by 4.5 (Cd), and 11.0 (Hg) kcal/mol, respectively.

It is clear that the energy barrier for DMA reacted with $[CdONO]^+$ is lower by around 11 kcal/mol compared to those for DMA reacting with NO_2^- (energy barrier: 42.1 kcal/mol [34]). The energy barrier for the reaction between DMA and $[HgONO]^+$ is not far from that for the nitrosation of DMA with NO_2^-. As shown in Figure 1, the first .step is the rate-limiting step with respect to the two metal components in the reaction. Comparing the energy barriers of the rate-limiting steps with the two metal components, the energy barriers decrease when Cd^{2+} is present, while no obvious changes occur if Hg^{2+} is added. As shown in Table 1, the free energy (ΔG_{298K}) associated with this pathway is 3.3 kcal/mol ($CdONO^+$) or 11.1 kcal/mol ($HgONO^+$). This suggests that Pathway 1 is more viable for $[CdONO]^+$ than for $[HgONO]^+$.

The natural atomic charges of the Entrance complex, TS1, Intermediate, and TS2 on Pathway 1 are illustrated in Figure S1 of the supporting information. As shown in Figure S1, the atomic charges of the metal atom are increasing from 0.88 (Cd) or 0.29 (Hg) for the Entrance complex to 1.43 (Cd) or 1.24 (Hg) for TS2. In TS2, the atomic charges of the oxygen atom, O(3) in Figure 1, are -1.31 ($CdONO^+$) or -1.15 ($HgONO^+$) which are about -0.9 lower than the corresponding values for the Entrance complex. The role of the metal atom in this pathway to provide electron density to the oxygen atom O(3) through the M–O(3) (M=Cd, Hg) bonds. This is important for the oxygen atom O(3) to abstract a hydrogen atom from DMA.

3.2 The Formation of NDMA from DMA and $[MONO]^+$(M=Cd, Pb, Hg), Pathway 2

As shown in Scheme 2, the second pathway of NDMA formation also involves two steps: the addition of DMA to $[MONO]^+$ forming an Intermediate, and the elimination of $[MOH]^+$. However, the transition state is very different from Pathway 1. The fully optimized structures of TS3, the Intermediate and TS4 as well as their relative energies are reported in Figure 2.

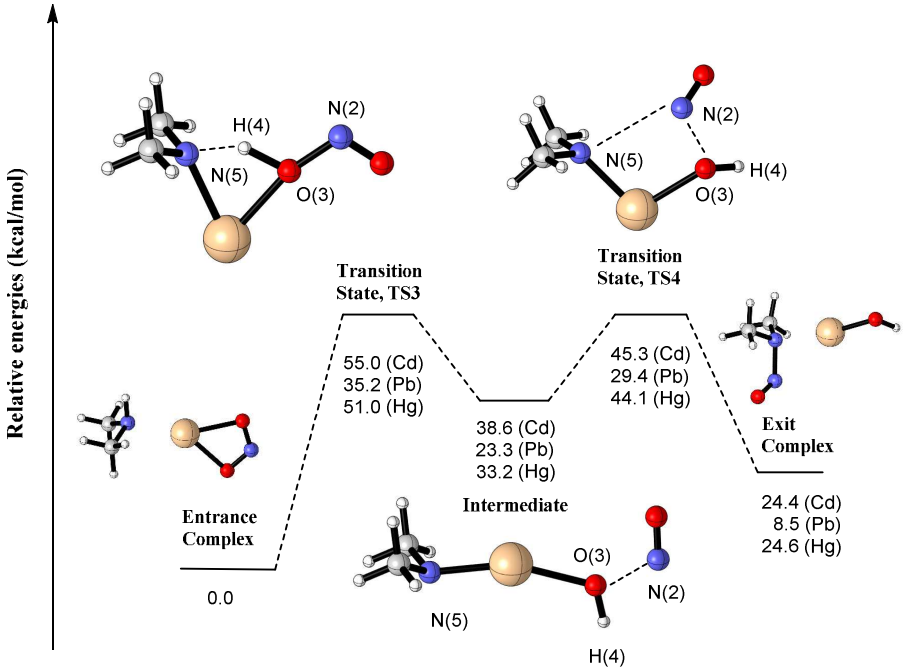

Figure 2 Stationary points on Pathway 2 of the DMA + $[MONO]^+$ (M=Cd, Pb, Hg) reaction

The first step of Pathway 2 is an addition reaction, starting from the complex of DMA with $[MONO]^+$ (M=Cd, Pb, Hg) forming transition state TS3 with C_s symmetry. In TS3, as shown in Figure 2, $[MONO]^+$ and DMA are connected through M–N(5) bonds

with lengths 2.26 Å (Cd), 2.21 Å (Pb) or 2.42 Å (Hg), respectively. The hydrogen atom H(4) from DMA connects oxygen atom O(3) from $[MONO]^+$, and the formed O(3)–H(4) separations are 1.17 Å (Cd), 1.11 Å (Pb), 1.20 Å (Hg), respectively. In the meantime, the N(5)–H(4) bond in DMA are elongated to 1.39 Å (Cd), 1.49 Å (Pb), 1.32 Å (Hg), suggesting that the interaction between H(4) and N(5) is weakened.

Following transition state TS3, an Intermediate will be produced. As shown in Figure 2, it is a complex consisting of NO attached to the $[(CH_3)_2N–MOH]^+$ fragment through the elongated N(2)–O(3) bond, for which distances are 1.75 Å (Cd), 1.72 Å (Pb) or 1.68 Å (Hg), respectively. The hydrogen atom H(4) has transferred to oxygen atom forming a genuine O(3)–H(4) bond with length ~0.97 Å. The distances between metal atom M (M=Cd, Pb, Hg) and atom N(5) are 2.11 Å (Cd), 2.06 Å (Pb) or 2.22 Å (Hg). The M–O(3) bond lengths are 2.23 Å (Cd), 2.38 Å (Pb) or 2.39 Å (Hg), respectively.

The next transition state TS4 will dissociate to $[M–OH]^+$ and NDMA as the final step of this pathway. In TS4, the N(2)–O(3) bond is elongated to 1.83 (Cd), 1.93 (Pb) or 1.88 Å (Hg), suggesting very weak interactions between M–OH and NO. The nitrogen atom from NO, namely N(2), approaches the nitrogen atom from DMA, namely N(5), with separations of 3.13 (Cd), 2.96 (Pb), and 2.37 Å (Hg), respectively.

Significantly, Figure 2 shows that the energy barriers for addition are slightly higher than those for Pathway 1 (barriers: 55.0 kcal/mol for $[CdONO]^+$, 35.2 kcal/mol for $[PbONO]^+$, 51.0 kcal/mol for $[HgONO]^+$). The energy barriers associated with the elimination reactions were computed to be 6.7, 6.1, and 10.9 kcal/mol, respectively.

Obviously, the addition reaction is the rate-determining step. Figure 2 also suggests that the energy barriers for the reactions of DMA with $[CdONO]^+$ or $[HgONO]^+$ are a little higher than those for DMA reacting with NO_2^- (42.1 kcal/mol [34]). The predicted free energy (ΔG_{298K}) for Pathway 2 is reported in Table 1; it is 7.5 kcal/mol for $[PbONO^+]$ but more than 20 kcal/mol for both $[CdONO]^+$ and $[HgONO]^+$. This indicates that the reaction of DMA with $[PbONO]^+$ may proceed *via* Pathway 2, but it is more difficult for the reaction of DMA with $[CdONO]^+$ or $[HgONO]^+$ to proceed *via* this pathway.

The natural atomic charges of the Entrance complex, TS3, Intermediate, and TS4 on Pathway 2 are reported in Figure S2 of the supporting information. As illustrated in Figure S2, the atomic charges of the metal atom in the Entrance complex are 1.35 (Cd), 1.48 (Pb), and 1.13 (Hg) respectively. In TS3, the metal atom bonds to the nitrogen atom in the DMA fragment, and its atomic charges change to 1.34 (Cd), 1.55 (Pb), and 1.07 (Hg). It seems that the Pb atom will donate electron density to oxygen atom O(3) and nitrogen atom N(5), and the Hg atom will accept electron density from both the N(5) and O(3) atoms. From the Intermediate to TS4, the atomic charges on the metal atoms are increasing by 0.03(Cd), 0.06(Pb) or 0.09(Hg). Considering the values of atomic charges on the O(3) atom in TS4, it seems that metal atom provides electron density to the O(3) through the M–O(3) bond.

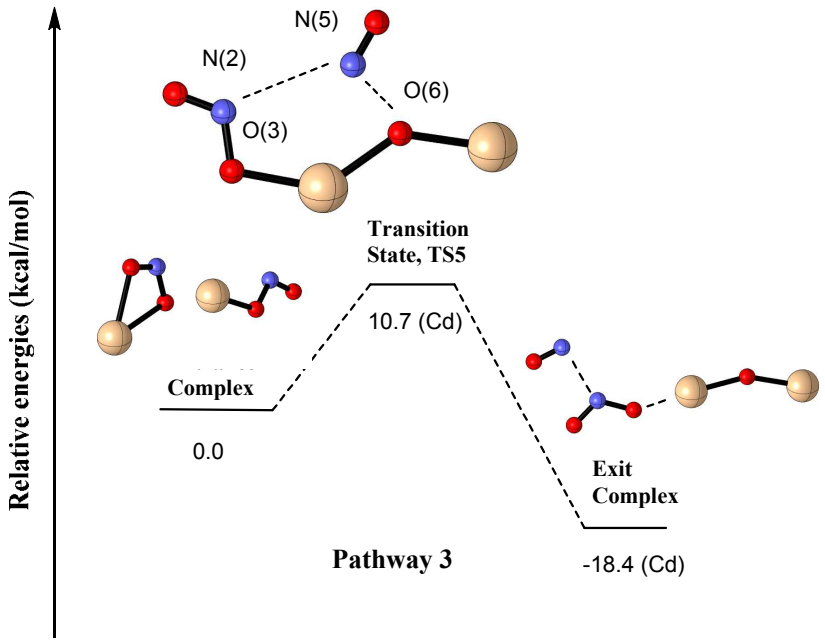

Figure 3 Stationary points on energy surface of reactions of two $[CdONO]^+$, Pathway 3

3.3 The Formation of N_2O_3 from $[CdONO]^+$ – Pathway 3

As shown in Figure 3, a new mechanism is proposed, namely the reaction of two molecules of $[CdONO]^+$ to give N_2O_3, which will react with DMA to generate NDMA *via* the release of HNO_2. For $[PbONO]^+$, the efforts to find a transition state TS5 failed. It appears that there is not a favorable pathway for $[PbONO]^+$. From the entrance complex $[HgONO]^+$, a transition state was obtained. However, it seems to lead to N_2O_4 instead of N_2O_3.

In the transition state TS5, as Figure 3 illustrated, one $[CdONO]^+$ molecule breaks into two parts, namely NO and $[CdO]^+$. The distances N(5)–O(6) are 1.89 Å, suggesting broken bonds. Simultaneously, both Cd atoms connect to atom O(6) , with bond lengths in the range of 2.10~2.14 Å. The distances between nitrogen atoms N(2) and N(5) are

3.12 Å, implying only a very weak interaction between them.

The natural atomic charges for the Entrance complex, and for TS5 on Pathway 3 are reported in Figure S3 of the supporting information. As shown in Figure S3, from the entrance complex to transition state TS5, the atomic charges of the two Cd atoms change from 1.37 and 1.60 to 1. 47 and 1.65. Since the predicted atomic charges on the oxygen atoms are -0.62, O(3), or -1.30 O(6), it may be concluded that electron density transfer takes place from the Cd atoms to oxygen atom O(3) and O(6) through the Cd–O bonds.

The energy barrier for N_2O_3 produced from $[CdONO]^+$ is predicted to be 10.7 kcal/mol. The formation of N_2O_3 from two molecules of $[CdONO]^+$ is exothermic by 18.4 kcal/mol. As shown in Table 1, the Gibbs free energy of this reaction in 298K is -17.7 kcal/mol. Thus the direct nitrosation of DMA by N_2O_3 should still be the leading pathway for the NDMA formation, due to its low energy barrier .

To conclude, the reaction between two molecules of $[CdONO]^+$ occurs easily, and Cd^{2+} may serve as an effective accelerator of the nitrosating agent N_2O_3. Therefore, the latter provides a feasible pathway (Figure 3) for the formation of NDMA in the "DMA + $[CdONO]^+$" reaction system. The catalytic effect of Cd^{2+} should not be ignored, for hazardous concentrations of NDMA in water are a real threat (the U.S. EPA suggests that a drinking water concentration of 0.7 ng L^{-1} for NDMA results in a 10^{-6} risk of contracting cancer). To our knowledge, no studies have directly aimed at the Cd^{2+}–catalyzed nitrosation of amine by NO_2^-. Further investigations should be carried out to check this possible catalysis due to Cd^{2+} and NO_2^- *in vitro* as well as *in vivo*.

Table 2, Energy barriers (kcal/mol) of three pathways obtained on PCM-B3LYP/ 6-311+G(d,p)/LANL2DZ level.

Reactions	Cd	Pb	Hg
Pathway 1, Entrace complex → Intermediate	23.8	-	3.3
Intermediate → Exit complex	4.0	-	4.6
Pathway 2, Entrace complex → Intermediate	42.8	43.1	33.6
Intermediate → Exit complex	4.8	5.3	-0.1
Pathway 3, Entrace complex → Exit complex	28.3	-	-

3.4 Effects of solvent

In order to discuss the effects of solvent, assuming the optimized geometries at the B3LYP/6-311+G(d,p)/LANL2DZ level, single-point energy computations were carried out at the same level of theory using a standard polarizable continuum model (PCM).[45] Water (ε=78.4) was selected to investigate the solvent effect on all three pathways. The energetics thus obtained are reported in Table 2.

As shown in Table 2, except for $[HgONO]^+$ in Pathway 1, the energy barriers in solvent are comparable the corresponding results in the gas phase. For Pathway 1, it seems that Cd^{2+} lowers the energy barriers (~20 kcal/mol) for the NDMA formation reaction from DMA and NO_2^- in water. Although the predicted energy barriers (Figure 1, ~42 kcal/mol) in the gas phase suggest that Pathway 1 will be difficult for $[HgONO]^+$, in water this pathway is more favorable for $[HgONO]^+$, considering its lower energy barrier (Table 2, 3.3 kcal/mol). For Pathway 2, it is suggested that $[HgONO]^+$ may proceed via this pathway, due to its relatively low energy barriers (Table 2, 33.6 kcal/mol), but may be more difficult for the reaction of DMA with $[CdONO]^+$ or $[PbONO]^+$ in water. For Pathway 3, it is shown that the energy barriers of $[CdONO]^+$ to give N_2O_3 in water are

~28 kcal/mol (Table 2). This is a possible NDMA formation pathway considering the low energy barrier for the next step in the formation process involving N_2O_3 and DMA.

4. Conclusions

NDMA has been demonstrated to be a probable potent human carcinogen. To better understand mechanisms of NDMA formation in the presence of heavy metal ions (specifically Cd^{2+}, Pb^{2+}, and Hg^{2+}), the reactions were investigated computationally.

The reaction of DMA with NO_2^- can be catalyzed by the heavy metal ions to form NDMA. The catalytic mechanism in neutral conditions involves one molecule of $[MONO]^+$ directly reacting with DMA to generate NDMA. This mechanism includes two steps: (1) the formation of an Intermediate from the reaction of DMA with $[MONO]^+$; (2) the formation of NDMA from the Intermediate. There are two different pathways to forming different transition states to catalyze the formation of NDMA. The studies in the gas phase suggest that $[CdONO]^+$ could lower the energy barriers for the NDMA formation reaction following Pathway 1. The predicted energy barriers for Pathway 2 show that $[PbONO]^+$ will catalyze the formation of NDMA.

Another catalytic mechanism obtained in the gas phase involves the reaction of two molecules of $[CdONO]^+$ to form the more reactive N_2O_3, followed by the reaction of N_2O_3 with DMA to form NDMA. In this mechanism Cd^{2+} can easily catalyze the formation of N_2O_3.

Considering solvent effects, the predicted energy barriers of Pathway 1 in water

involving DMA and $[CdONO]^+$ or $[HgONO]^+$ are lower than in the gas phase. For Pathway 2, the NDMA formation process will be catalyzed in water by $[HgONO]^+$. The energy barriers for Pathway 2 involving $[PbONO]^+$or $[CdONO]^+$ are ~43 kcal/mol. The energy barriers predicted in solvent for Pathway 3 are consistent with the corresponding results in the gas phase.

We hope these results will help further elucidate nitrosation mechanisms and are also helpful for the search of new inhibitors and methods to prevent the formation of hazardous nitrosamine.

5. Acknowledgments

This work was supported by the U.S. National Science Foundation, Grant CHE-1361178, the National Natural Science Foundation of China (No. 20903006), and the Beijing Natural Science Foundation (No. 2092008). Y L acknowledges financial support from the China Scholarship Council. We thank Professor Guoliang Li of South China Normal University for helpful discussions.

References

[1] P. N. Magee, J. M. Barnes, *J. Cancer* , 1956, **10**, 114.

[2] L. M. Anderson, V. L. Souliotis, S. K. Chhabra, T. J. Moskal, S. D. Harbaugh, S. A. Kyrtopoulos, *Int. J. Cancer* , 1996, **66**, 130.

[3] I. V. Mizgireuv, I. G. Majorova, V. M. Gorodinskaya, V. V. Khudoley, S. Y. Revskoy, *Toxicol. Pathol.* , 2004, **32**, 514.

[4] S. Fukushima, H. Wanibuchi, K. Morimura, D. Nakae, H. Tsuda, K. Imaida, T. Shirai, M. Tatematsu, T. Tsukamoto, M. Hirose and F. Furukawa, *Cancer Lett.*, 2005, **222**, 11

[5] N. P. Sen, S. Seaman and W. F. Miles, *J. Agr. Food Chem.*, 1979, **27**, 1354.

[6] G. Stehlik, O. Richter and H. Altmann, *Ecotox. Environ. Safe.*, 1982, **6**, 495.

[7] B. Spiegelhalder and R. Preussmann, *J. Cancer Res. Clin.*, 1984, **108**, 160.

[8] W. A. Mitch, J. O. Sharp, R. R. Trussell, R. L. Valentine, L. Alvarez-Cohen and D. L. Sedlak, *Environ. Eng. Sci.*, 2003, **20**, 389.

[9] S. W. Krasner, W. A. Mitch, D. L. McCurry, D. Hanigan and P. Westerhoff, *Water Res.*, 2013, **47**, 4433.

[10] D. A. Shah and W. A. Mitch, *Environ. Sci. Technol.*, 2012, **46**, 119.

[11] J. Choi and R. L. Valentine, *Water Res.*, 2002, **36**, 817.

[12] W. A. Mitch and D. L. Sedlak, *Environ. Sci. Technol.*, 2002, **36**, 588.

[13] I. M. Schreiber and W. A. Mitch, *Environ. Sci. Technol.*, 2005, **39**, 3811.

[14] I. M. Schreiber and W. A. Mitch, *Environ. Sci. Technol.*, 2006, **40**, 6007.

[15] J. Choi and R. L. Valentine, *Environ. Sci. Technol.*, 2003, **37**, 4871.

[16] P. Andrzejewski, B. Kasprzyk-Hordern and J. Nawrocki, *Water Res.*, 2008, **42**, 863.

[17] L. Yang, Z. Chen, J. Shen, Z. Xu, H. Liang, J. Tian, Y. Ben, X. Zhai, W. Shi and G. Li, *Environ. Sci. Technol.*, 2009, **43**, 5481.

[18] I. M. Schreiber and W. A. Mitch, *Environ. Sci. Technol.*, 2007, **41**, 7039.

[19] L. P. Padhye, B. Hertzberg, G. Yushin and C. Huang, *Environ. Sci. Technol.*, 2011, **45**, 8368.

[20] F. Soltermann, M. Lee, S. Canonica and U. Von Gunten, *Water Res.*, 2013, **47**, 79.

[21] M. Liang, W. Li, Q. Qi, P. Zeng, Y. Zhou, Y. Zheng, M. Wu and H. Ni, *RSC Advances*, 2016, **6**, 5677.

[22] P. G. Wang, M. Xian, X. Tang, X. Wu, Z. Wen, T. Cai and A. J. Janczuk, *Chem. Rev.*, 2002, **102**, 1091.

[23] S. S. Mirvish, *Toxicol. Appl. Pharm.*, 1975, **31**, 325.

[24] Y. Huang, J. Ji and Q. Hou, *Mutat. Res.*, 1996, **358**, 7.

[25] K. Ohsawa, S. Nakagawa, M. Kimura, C. Shimada, S. Tsuda, K. Kabasawa, S. Kawaguchi and Y. F. Sasaki, *Mutat. Res.*, 2003, **539**, 65.

[26] C. A. Krul, M. J. Zeilmaker, R. C. Schothorst and R. Havenaar, *Food Chem. Toxicol.*, 2004, **42**, 51.

[27] M. J. Zeilmaker, M. I. Bakker, R. Schothorst and W. Slob, *Toxicol. Sci.*, 2010, **116**, 323.

[28] C. L. Lv, Y. D. Liu and R. Zhong, *J. Phys. Chem. A,* 2008, **112**, 7098.

[29] Y. Zhao, S. L. Garrison, C. Gonzalez, W. D. Thweatt and M. Marquez, *J. Phys. Chem. A,* 2007, **111**, 2200.

[30] D. Trogolo, B. K. Mishra, M. B. Heeb, U. Gunten and J. S. Arey, *Environ. Sci. Technol.*, 2015, **49**,

4163.
[31] W. Gan, T. Bond, X. Yang and P. Westerhoff, *Environ. Sci. Technol.*, 2015, **49**, 11429.
[32] L. K. Keeper and P. P. Roller, *Science*, 1973, **181**, 1245.
[33] C. L. Lv, Y. D. Liu, R. Zhong and Y. Wang, *J. Mol. Struct.* 2007, **802**, 1.
[34] Z. Sun, Y. D. Liu and R. G. Zhong, *J. Phys. Chem. A,* 2011, **115**, 7753.
[35] H. Zhang and S. A. Andrews, *Chemosphere*, 2013, **93**, 2683.
[36] Z. Wang and W. A. Mitch, *Environ. Sci. Technol.*, 2015, **49**, 11974.
[37] R. K. Sharma, M. Agrawal and F. M. Marshall, *Food Chem. Toxicol.*, 2009, **47**, 583.
[38] A. D. Becke, *J. Phys. Chem.*,1993, **98**, 5648.
[39] C. Lee, W. Yang and R. G. Parr, *Phys. Rev. B*, 1988, **37**, 785.
[40] A. D. McLean and G. S. Chandler, *J. Chem. Phys.,* 1980, **72**, 5639.
[41] R. Krishnan, J. S. Binkley, R. Seeger and J. A. Pople, *J. Chem. Phys.,* 1980, **72**, 650.
[42] P. J. Hay and W. R. Wadt, *J. Chem. Phys.,* 1985, **82**, 299.
[43] A. E. Reed, R. B. Weinstock, and F. Weinhold, *J. Chem. Phys.*, 1985, **83,** 735.
[44] Gaussian 09 (Revision A.01), M. J. Frisch, G. W. Trucks, H. B. Schlegel, G. E. Scuseria, M. A. Robb, J. R. Cheeseman, G. Scalmani, V. Barone, B. Mennucci, G. A. Petersson, H. Nakatsuji, M. Caricato, X. Li, H. P. Hratchian, A. F. Izmaylov, J. Bloino, G. Zheng, J. L. Sonnenberg, M. Hada, M. Ehara, K. Toyota, R. Fukuda, J. Hasegawa, M. Ishida, T. Nakajima, Y. Honda, O. Kitao, H. Nakai, T. Vreven, J. A. Montgomery, Jr., J. E. Peralta, F. Ogliaro, M. Bearpark, J. J. Heyd, E. Brothers, K. N. Kudin, V. N. Staroverov, R. Kobayashi, J. Normand, K. Raghavachari, A. Rendell, J. C. Burant, S. S. Iyengar, J. Tomasi, M. Cossi, N. Rega, J. M. Millam, M. Klene, J. E. Knox, J. B. Cross, V. Bakken, C. Adamo, J. Jaramillo, R. Gomperts, R. E. Stratmann, O. Yazyev, A. J. Austin, R. Cammi, C. Pomelli, J. W. Ochterski, R. L. Martin, K. Morokuma, V. G. Zakrzewski, G. A. Voth, P. Salvador, J. J. Dannenberg, S. Dapprich, A. D. Daniels, Ö. Farkas, J. B. Foresman, J. V. Ortiz, J. Cioslowski, D. J. Fox, Gaussian, Inc., Wallingford, CT, **2009**.
[45] J. Tomasi, B. Mennucci, and R. Cammi, *Chem. Rev.*, 2005, **105**, 2999.